A Combined Spectroscopic and Theoretical Study of a Series of Conformationally Restricted Hexapeptides Carrying a Rigid Binaphthyl–Nitroxide Donor–Acceptor Pair

Basilio Pispisa,*[a] Claudia Mazzuca,[a] Antonio Palleschi,[a] Lorenzo Stella,[a] Mariano Venanzi,[a] Michel Wakselman,[b] Jean-Paul Mazaleyrat,[b] Mario Rainaldi,[c] Fernando Formaggio,[c] and Claudio Toniolo[c]

Abstract: The structural features of a series of linear hexapeptides of general formula Boc-B-A_r-T-A_m-O*t*Bu, where A is L-Ala or Aib (α-aminoisobutyric acid), B is (*R*)-Bin, a binaphthyl-based $C^{\alpha,\alpha}$-disubstituted Gly residue, T is Toac, a nitroxide spin-labeled $C^{\alpha,\alpha}$-disubstituted Gly, and $r+m=4$, were investigated in methanol solution by fluorescence, transient absorption, IR and CD spectroscopic studies, and by molecular mechanics calculations. These peptides are denoted as B-T/r-m, to emphasize the different position of Toac with respect to that of the Bin fluorophore in the amino acid sequence. The rigidity of the B-T donor–acceptor pair and of the Aib-rich backbone allowed us to investigate the influence of the interchromophoric distance and orientation on the photophysics of the peptides examined. The excited state relaxation processes of binaphthyl were investigated by time-resolved fluorescence and transient absorption experiments. Dynamic quenching of the excited singlet state of binaphthyl by Toac was successfully interpreted by the Förster energy transfer model, provided that the mutual orientation of the chromophores is taken into account. This implies that interconversion among conformational substates, which involves puckering of the Toac piperidine ring, is slow on the time scale of the transfer process, that is slower than 5 ns. By comparison of the experimental and theoretical data, the type of secondary structure (right-handed 3_{10} helix) from the B-T/*r-m* peptides in solution was determined; this would not have been achievable by using the CD and NMR data only, as the data are not diagnostic in this case. Static quenching was observed in all peptides examined but B-T/1-3, where the effect can be ascribed to a non-fluorescent complex. Among the computed low-energy conformers of these peptides, there is one structure exhibiting a NO$^{\cdot}$–naphthalene center-to-center distance <6 Å, which might be assigned to this complex. The overall results emphasize the versatility of fluorescence experiments in 3D-structural studies in solution.

Keywords: amino acids · atropisomerism · conformation analysis · molecular dynamics · time-resolved spectroscopy

Introduction

Protein–protein and protein–nucleic acid interactions are important naturally occurring processes,[1] which involve helical structural segments of both partners. This explains the current remarkable interest in both model peptides containing amino acids with a high helix propensity, such as $C^{\alpha,\alpha}$-disubstituted Gly residues,[2] and conformational equilibria involved. A rapid identification of the most relevant 3D-structural features of the peptides in solution is thus a significant aspect of their investigation and of their intermolecular interactions in general. Time-resolved fluorescence spectroscopy represents a valuable tool in tackling this problem, provided that the compounds under investigation carry appropriate chromophores. Nitroxyl radicals are therefore widely employed to probe the structural and dynamical features of biological materials, such as membranes, proteins and micelles;[3–6] they are also employed to test the reactivity of hemo- and iron-sulfur proteins.[7] Despite the wide interest in nitroxyl radicals, the mechanism by which excited states of aromatic molecules are quenched by paramagnetic species still remains to be solved. Electron exchange interactions,

[a] Prof. B. Pispisa, Dr. C. Mazzuca, Prof. A. Palleschi, Dr. L. Stella, Prof. M. Venanzi
Dipartimento di Scienze e Tecnologie Chimiche
Università di Roma Tor Vergata, 00133 Roma (Italy)

[b] Dr. M. Wakselman, Dr. J.-P. Mazaleyrat
SIRCOB, UMR CNRS 8086, Bât. Lavoisier
Université de Versailles, 78035 Versailles (France)

[c] Dr. M. Rainaldi, Prof. F. Formaggio, Prof. C. Toniolo
Istituto di Chimica Biomolecolare, C.N.R.
Dipartimento di Chimica Organica, Università di Padova
35131 Padova (Italy)

DOI: 10.1002/chem.200304727

which enhance internal conversion to the ground state, were invoked to explain the photophysics of a series of covalently linked nitroxide/fluorophore compounds, with interchromophoric distances in the range of 6 – 9 Å.[8] Exchange interactions were reported to predominate in the intermolecular quenching of freely diffusing donor – acceptor systems comprising a nitroxide quencher,[4] because a strong electronic coupling and overlap of electronic distributions are required for such short-range mechanism. By contrast, in covalently linked donor – acceptor systems, particularly where the photophysical probes are separated by rigid spacers, long-range electron transfer[3c] and Förster energy transfer[3b, 9] were found to be important. Spectral measurements showed that Förster transfer mechanism extends the nitroxide quenching radius to as much as 10 Å.[10]

On the other hand, the relevant charge-transfer character of the binaphthyl excited states and the strong exciton coupling between the two naphthyl moieties have been extensively investigated.[9, 11] In addition, 1,1′-binaphthyl derivatives were employed as rigid fluorophores in photophysical studies,[11] and as homogeneous catalysts in asymmetric reactions.[12a] They were also used for tailoring new materials,[12b] such as chiral hosts in molecular recognition processes.

We present here a structural study, based on spectroscopic and theoretical data, on a series of conformationally restricted hexapeptides carrying both a nitroxide derivative and a binaphthyl group. The presence of Aib (α-aminoisobutyric acid) residues in the main chain leads to ordered secondary structures because of its high helix-forming propensity, as a result of the steric constraints of the *gem*-dimethyl group.[2c,d, 13] The general formula of these peptides is Boc-B-A_r-T-A_m-O*t*Bu (Boc: *tert*-butyloxycarbonyl, O*t*Bu: *tert*-butoxy, A: L-Ala or Aib, B: (*R*)-Bin, i.e., 4,5-dihydro-4-amino-3*H*-cyclohepta[2,1-*a*:3,4-*a*′]}dinaphthalene-4-carboxylic acid, T: Toac, i.e., 2,2,6,6-tetramethyl-piperidine-1-oxyl-4-amino-4-carboxylic acid; $r+m=4$) as shown below. The peptides are here denoted as B-T/*r*-*m*, that is B-T/0-4, B-T/1-3, B-T/2-2 and B-T/3-1, thus emphasizing the length of the spacer between the chromophores in the backbone chain.

Boc - B - A_r - T - A_m - O*t* Bu:

Boc-**B**-**T**-Ala-Aib-Aib-Ala-O*t*Bu: **B-T/0-4**

Boc-**B**-Aib-**T**-Ala-Aib-Ala-O*t*Bu: **B-T/1-3**

Boc-**B**-Aib-Ala-**T**-Aib-Ala-O*t*Bu: **B-T/2-2**

Boc-**B**-Aib-Aib-Ala-**T**-Ala-O*t*Bu: **B-T/3-1**

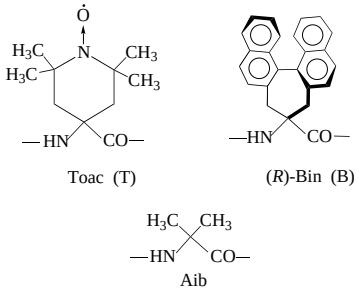

The aim of the work was two-fold. First, to clarify the conformational features of these sterically restricted peptides. Second, to study the influence of the fixed spatial orientation and distance of the chromophores on the photophysics of these compounds, for gaining a better insight into the relaxation process within the D – A pair. In fact, the rigidity of the overall structure makes it easier to compare the experimental parameters with those theoretically obtained by molecular mechanics.

A preliminary account of this research has already been reported,[14] but we now present a thorough investigation based on the combination of fluorescence and computational data. In addition, the findings indicate that the secondary structure attained by the B-T/*r*-*m* peptides in solution is a right-handed 3_{10} helix, a result not easily achievable when as in the present case the CD and NMR spectra are not informative.[15, 16] Finally, we also discuss the origin of the observed static quenching in all peptides examined, but B-T/1-3, suggesting that a non-fluorescent complex forms, in which an instantaneous process between the active chromophores takes place.

Results and Discussion

UV, CD and IR Spectra: The UV absorption spectra of both the reference Boc-(*R*)-Bin-O*t*Bu, containing only the binaphthyl moiety, and the B-T/*r*-*m* hexapeptides in methanol solution exhibit a shift to 305 nm of the naphthalene ^1L_a transition band, usually observed at around 280 nm, while the band at around 225 nm (^1B_b) is split, the absorption maxima falling at 218 and 230 (sh) nm. This finding indicates a strong electronic coupling between the two ^1B_b transitions, located on the different naphthalene rings, through intramolecular exciton interaction. This leads to a reduction of the HOMO – LUMO energy gap, in agreement with the bathochromic shift of the lowest energy absorption band. Accordingly, the CD spectra in the far-UV region, characteristic of the *R* configuration of binaphthyl,[17] exhibits an exciton splitting clearly ascribable to the aforementioned coupling regime, as shown in Figure 1. Within the same wavelength

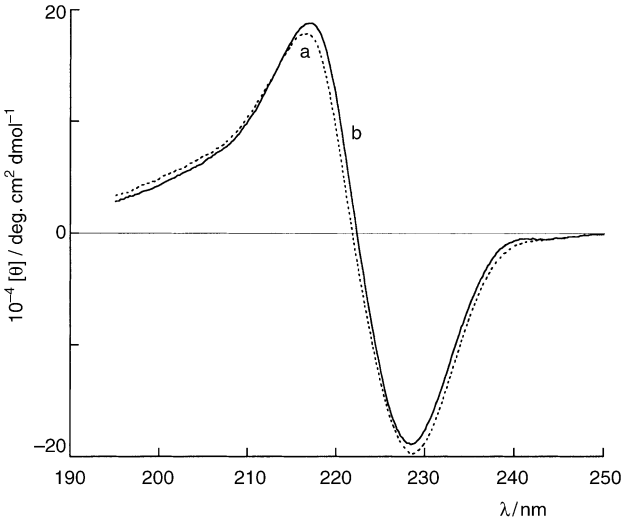

Figure 1. CD spectra of the reference Boc-(*R*)-Bin-O*t*Bu (a), B-T/0-4 (b) in methanol solution; peptide concentration 10^{-3} M.

region (190–250 nm), the contributions of the Bin[17] and Toac[18] chromophores to the overall ellipticity strongly overlap with that of the peptide chromophore,[19] so that no useful information about the kind of secondary structure of the hexapeptides could be obtained with this technique.

FT-IR absorption spectra of the hexapeptides in $CDCl_3$ were carried out in a concentration range of 10^{-2}–10^{-4} M (Figure 2). Helical peptides exhibit two characteristic absorption bands in the NH stretching region, one around 3430 cm^{-1},

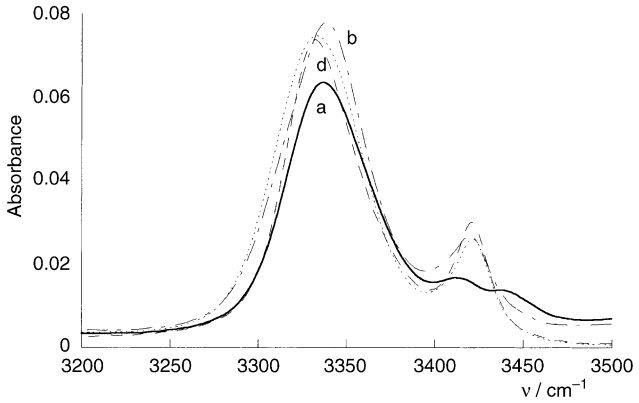

Figure 2. FT-IR absorption spectra in the NH stretching region of B-T/0-4 (a), B-T/1-3 (b), B-T/2-2 (c) and B-T/3-1 (d) in $CDCl_3$. Peptide concentration $\approx 10^{-3}$ M.

associated to the NH groups not involved in hydrogen-bond interactions, and the other at around 3330 cm^{-1}, typical of hydrogen-bonded NH groups.[20, 21] We measured the ratio of the integrated intensities of the transitions of hydrogen-bonded (A_b) and free (A_f) NH groups, normalized for the appropriate extinction coefficients according to the expression $n_b/n_f = (A_b/A_f)/(\varepsilon_b/\varepsilon_f)$,[22] where n is the number of peptide units, and ε the integrated molar extinction coefficient, subscripts b and f denoting hydrogen-bonded and free NH groups, respectively. The value of the n_b/n_f ratio is, on the average, 1.8 ± 0.3 for all peptides examined but B-T/0-4; this value is in good agreement with the theoretical value of 2, calculated for a hexapeptide in 3_{10}-helical conformation with a $i+3 \leftarrow i$ (C_{10}) hydrogen-bonding scheme.

The IR absorption of B-T/0-4 shows a doublet within the frequency region of 3410–3440 cm^{-1} (Figure 2a), which implies the presence of two free NH groups in a different environment. Noteworthy the molecular mechanics results account for this finding, such that the deepest energy minimum structure of this peptide exhibits two hydrogen-bond free NH groups, differently exposed to the environments.

The IR results described above suggest that the hexapeptides investigated largely populate a 3_{10} helix in solution. This conclusion agrees with earlier results on a related hexapeptide, but with (*S*)-Bin and Toac as the donor–acceptor pair, for which the structural features were fully characterized by X-ray diffraction in the crystal state.[11]

Steady-state and time-resolved fluorescence: Steady-state fluorescence experiments of the hexapeptides in methanol solution show a substantial quenching of the Bin emission by Toac, as illustrated in Figure 3. The fluorescence quantum yields (Φ) are reported in Table 1, together with the efficiencies of the quenching process, E, as given by $[1-(\Phi/\Phi_0)]$, where Φ_0 is the quantum yield of the reference derivative

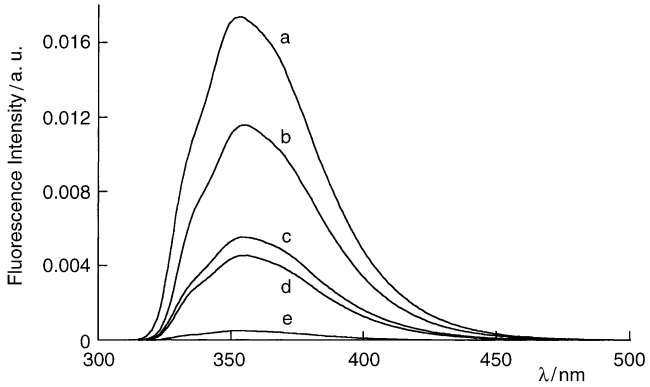

Figure 3. Steady-state fluorescence spectra of the reference Boc-(*R*)-Bin-O*t*Bu (a), B-T/1-3 (b), B-T/0-4 (c), B-T/3-1 (d) and B-T/2-2 (e) in methanol.

Table 1. Quantum yields and steady-state quenching efficiencies of B-T/*r-m* hexapeptides in methanol.[a]

Peptide	Φ	E
B-T/0-4	0.23	0.68
B-T/1-3	0.47	0.34
B-T/2-2	0.02	0.97
B-T/3-1	0.18	0.74

[a] $\lambda_{ex} = 305$ nm.

Boc-(*R*)-Bin-O*t*Bu. No evidence for exciplex emission could be obtained, even upon decreasing the solvent polarity (dioxane).

We next investigated the time-resolved fluorescence ($\lambda_{ex} = 305$, $\lambda_{em} = 360$ nm). The time decay curve of the reference is well described by a single lifetime ($\tau_0 = 4.8$ ns), while the time decays of all B-T/r-m peptides are fitted by a multiexponential function [Eq. (1)],[23]

$$I(t) = \Sigma_i \alpha_i \exp(-t/\tau i) \quad (1)$$

as shown in Figure 4, where the fluorescence decays of B-T/1-3 and B-T/2-2 in methanol are reported. Table 2 lists the lifetimes, preexponents and quenching efficiencies of B-T/*r-m*, these latter being given by Equation (2):

$$E_i = 1 - (\tau_i/\tau_0) \quad (2)$$

In Table 2 the same parameters from the distribution analysis of the experimental decays are also reported. This analysis does not include any specific decay model, but only gives the relative weights of a continuum of lifetimes.[23] From the results, it appears that all peptides exhibit narrow distributions, the average lifetimes and relative weights being fully consistent with those of the discrete model. An unfolded peptide, which is characterized by a random distribution of donor–acceptor distances, would have led to a broad

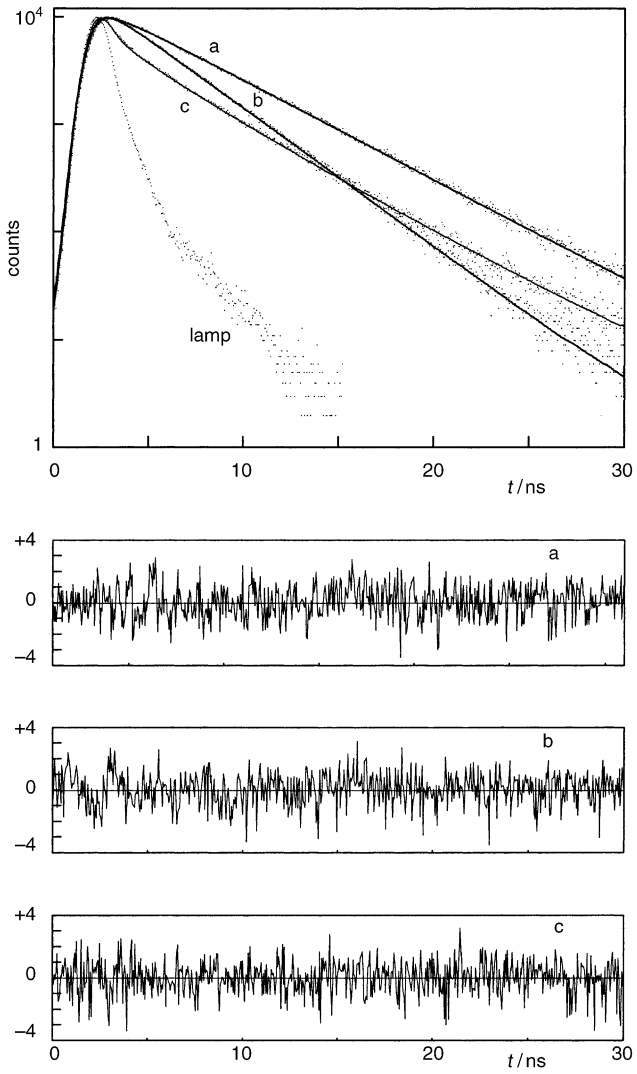

Figure 4. Typical example of fluorescence decay curves: Boc-(*R*)-Bin-O*t*Bu (a), B-T/1-3 (b) and B-T/2-2 (c) in methanol ($\lambda_{ex}=305$, $\lambda_{em}=360$ nm). The full lines represent the best fit to the experimental data. The lamp profile and the residuals are also shown.

distribution of lifetimes. Therefore, the data reported in Table 2 strongly suggest that all peptides in the series considered are highly organized in a structure supporting solvent such as methanol, in agreement with the IR results. In addition, it is reasonable to assign each decay component to one single conformer.[22, 23]

The observation that $\langle\tau\rangle/\tau_0 \neq \Phi/\Phi_0$ for all peptides examined, except for B-T/1-3, where $\langle\tau\rangle = \Sigma_i \alpha_i \tau_i$ suggests that static quenching does occur; the effect arises from an instantaneous process within a complex between the active chromophores. For instance, $\langle\tau\rangle/\tau_0 = 0.30 \pm 0.06$ and 0.62 ± 0.06, compared with $\Phi/\Phi_0 = 0.03 \pm 0.01$ and 0.26 ± 0.02 for B-T/2-2 and B-T/3-1, respectively. By contrast, for B-T/1-3 $\langle\tau\rangle/\tau_0 = 0.67$ and $\Phi/\Phi_0 = 0.66$. It is worth anticipating that in this latter case the steric arrangement of Toac and Bin in the low-energy conformers is such as to prevent any instantaneous process between the chromophores, because they are lying on the opposite side of the 3_{10} helix.

Table 2. Time decay parameters of excited Bin in the (*R*)-Bin/Toac peptides in methanol from both exponential (ex) and lifetimes distribution (ld).[a]

Peptide	Data analysis	α_1	τ_1 [ns]	E_1	α_2	τ_2 [ns]	E_2	χ^2
B-T/0-4	ex	0.65	0.74	0.84	0.35	4.83	0.00	1.03
	ld	0.61	0.71	0.85	0.39	4.73	0.01	1.00
B-T/1-3	ex	0.12	1.81	0.62	0.88	3.43	0.28	1.10
	ld	0.06	1.93	0.60	0.94	3.35	0.30	0.93
B-T/2-2	ex	0.74	0.47	0.90	0.26	4.36	0.09	1.13
	ld	0.69	0.43	0.91	0.31	4.16	0.13	1.17
B-T/3-1	ex	0.70	2.55	0.47	0.30	4.02	0.16	1.02
	ld	0.88	2.80	0.41	0.12	4.56	0.04	1.09

[a] $\lambda_{ex}=305$ nm, $\lambda_{em}=360$ nm. The uncertainty in lifetimes is around 5% for the long component and around 10% for the short one. The uncertainty in the pre-exponents is around 10%.

To summarize, fluorescence measurements made it possible to experimentally establish the presence of non-fluorescent conformers in solution. The complexity of the UV/Vis absorption spectra is such as to veil any relatively small perturbation ascribable to these non-fluorescent complexes.

Transient absorption measurements: To further investigate the nature of the Bin–Toac interaction we performed transient absorption experiments within the 300–500 nm wavelength region with nanosecond time resolution. For all peptides examined, only signals ascribable to the binaphthyl triplet–triplet absorption are observed ($\lambda_{max} \approx 415$ nm in methanol). The lack of signals from transient radical species rules out the occurrence of an electron transfer process involving the binaphthyl and the nitroxide chromophores in the ns–μs time range. In Figure 5, a typical transient

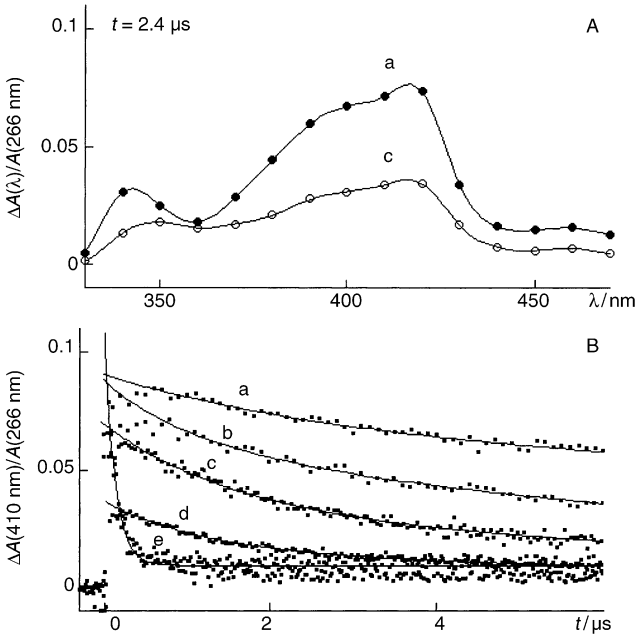

Figure 5. A) Typical nanosecond transient absorption spectra of binaphthyl triplet ($t=2.4\,\mu$s after excitation): Boc-(*R*)-Bin-O*t*Bu (a) and B-T/0–4 (c). B) Transient absorption decays ($\lambda=410$ nm) of Boc-(*R*)-Bin-O*t*Bu (a), B-T/1-3 (b), B-T/0-4 (c), B-T/3-1 (d) and B-T/2-2 (e). The solid lines represent the exponential fit to the experimental data.

absorption spectrum of the hexapeptides in methanol is reported, together with that of the reference. In the same Figure, the T–T absorption time decays, normalized for the absorption at the laser pump excitation wavelength, $[\Delta A(t)/A(266)]$, are shown. From the results, both the normalized differential absorption at $t=0$, $\Delta A(0)/A$, which is proportional to the triplet state population, and the rate constant of the triplet state depletion, k_T, were obtained, as reported in Table 3. With the only exception of B-T/2-2, the $\Delta A(0)/A$ values qualitatively follow the same trend of the singlet state quenching efficiency, probably because of the competition between the energy transfer (ET) and the singlet–triplet intersystem crossing (ISC) processes. However, the values of $\Delta A(0)/A$ are higher than those expected for a pure ET/ISC competition from the excited singlet state. This is particularly true for the B-T/2-2 peptide, for which the $\Delta A(0)/A$ value exceeds even that of the reference. This finding suggests that an enhanced intersystem crossing (EISC) process does take place, very likely ascribable to the instantaneous interaction within a complex in which a mechanism primarily controlled by short-range exchange interactions occurs. This hypothesis is consistent with both the occurrence of the observed static fluorescence quenching and the results previously reported for the interaction between aromatic molecules and stable free radicals.[24] The reason why the EISC effect is larger in B-T/2-2 than in the other peptides is that its fraction of non-fluorescent complex is the largest among all compounds examined (see below).

Table 3. Triplet state amplitude and rate constants from transient absorption experiments in methanol.

Peptide	$\Delta A(0)/A$[a]	$[\Delta A(0)/A]/[\Delta A(0)/A]_{Bin}$	$10^{-5}k_T$[b] [s^{-1}]	E_T[c]
Bin	0.091	–	0.71	–
BT/0-4	0.072	0.70	2.8	0.75
BT/1-3	0.087	0.95	1.1	0.33
BT/2-2	0.108	1.18	83.0	0.99
BT/3-1	0.036	0.40	3.0	0.77

[a] Differential absorption at $t=0$, normalized for the absorption at $\lambda=$ 266 nm. [b] Rate constant of triplet decay. [c] From Equation (3).

As far as the k_T rate constants are concerned, they are directly related to the photophysical processes depleting the triplet excited states population. We can therefore introduce the triplet quenching efficiency E_T as in Equation (3):

$$E_T = 1 - (k_T^0/k_T) \quad (3)$$

where k_T^0 is the decay rate constant of the reference. The values of E_T nicely parallel the singlet state quenching efficiencies, that is, B-T/2-2 > B-T/3-1 ≈ B-T/0-4 > B-T/1-3, confirming the idea that stable free radicals are able to quench both singlet and triplet states of aromatic molecules.[25] Therefore, both long range dipole–dipole and short-range exchange interactions not only contribute to the overall singlet state quenching, but also control the triplet state decay.

Very recently,[26] the triplet state relaxation of a series of functionalized peptides, carrying several aromatic moieties (binaphthyl, benzophenone, trypthophan) and a nitroxide quencher as donor–acceptor pairs, were studied by time-resolved EPR experiments. Electron-exchange interactions were reported to be primarily responsible for the triplet state quenching of the aromatic molecules (EISC to the ground state) and for the generation of Toac spin polarization, induced by spin selective mixing of doublet and quartet. In addition, exchange interactions were thought to affect the singlet state relaxation, even though it was impossible to discriminate between energy transfer and electron-exchange contributions of the singlet state quenching. According to our results described above, the combined approach of flash photolysis and time-resolved fluorescence experiments allows us to characterize both processes and the way in which they affect both the singlet and triplet excited states decay mechanisms.

Computational results and molecular modeling: We now address specific questions regarding the 3D-structural features of the hexapeptides examined in methanol solution, that is i) which type of secondary structure they populate, ii) which conformational equilibria predominate in the time scale region of our measurements, and iii) which geometric and steric constraints control the distance and orientation of the Bin/Toac pair. To answer these questions, molecular mechanics calculations[27, 28] were carried out, starting by putting the backbone chain in both left-handed (l.h.) and right-handed (r.h.) 3_{10} and α helices. This approach was used for two reasons, namely i) because the handedness of the secondary structure could not be determined by CD measurements (see above), and ii) because earlier X-ray diffraction results on an analogous hexapeptide, but carrying (*S*)-Bin, showed that it attains a left-handed, not a right-handed 3_{10} helix, as one would have expected from the presence of L-Ala residues in the backbone.[11]

For each peptide the total potential energy of electrostatic (COUL), nonbonding (NB), hydrogen-bond (HB) and torsional (TOR) interactions was calculated by using standard bond angles and bond lengths.[29] Nonbonded interatomic interactions were evaluated by a 6-12 Lennard-Jones potential function, and hydrogen-bond interactions by a dipole–dipole function, D/r^3, where $D = -230.1$ kJ mol^{-1} Å^3.[27a] Coulombic interactions were assessed by assigning partial atomic charges for each atom in the peptides and using a distance-dependent dielectric constant. Finally, a threefold torsional potential function, with barriers $V_0 = 5.0$ and 11.7 kJ mol^{-1} for rotation around the N–C and C–C bonds, was adopted. Energy minimization refinement was eventually performed by relaxing the fixed geometry for all internal degrees of freedom, including those of the ordered backbone chain, by making use of Equation (4), also comprising stretching and bending terms (STR and BEN).[22, 27b]

$$U_m = \mathrm{COUL} + \mathrm{HB} + \mathrm{NB} + \mathrm{TOR} + \mathrm{STR} + \mathrm{BEN} \quad (4)$$

The answer to the first question is that all low-energy conformers of B-T/r-m peptides populate a right-handed 3_{10} helix, as shown in Table 4 for B-T/2-2, where the value of U_m for the right-handed 3_{10}-helical conformers appears to be

Table 4. Relative energy of the sterically most favored conformers of B-T/2-2 with different secondary structure and quenching efficiencies.

Type of helix	U_m[a]	R_m[b]	E_m[c]	E_i[d]
r.h. 3_{10} helix	0.00	6.32	0.83	
	0.19	7.23	0.87	0.90, 0.09
	0.50	7.26	0.14	
l.h. 3_{10} helix	3.1	9.60	0.40	
	4.5	8.52	0.62	
r.h. α helix	1.7	6.91	0.82	
l.h. α helix	2.3	6.01	0.78	

[a] kcal mol^{-1}, from Eq. (4). [b] Interchromophoric center-to-center distance [Å]. [c] Calculated quenching efficiency, from Eq. (5). [d] Experimental quenching efficiency, from Eq. (2).

lower by more than 3 kcal mol^{-1} than that of the left-handed 3_{10} helix, and by more than 1.5 kcal mol^{-1} than that of right- or left-handed α helix. This finding is validated by the very good agreement between experimental and calculated quenching efficiencies observed only with the right-handed 3_{10}-helical conformers. The calculated efficiency was obtained by applying the Förster model of energy transfer.[27] Noteworthy the correlation between calculated and experimental efficiency is highly demanding in terms of structural features, because the quenching efficiency depends on the sixth power of the interprobe distance and on the mutual orientation of the probes, besides the spectroscopic parameter R_0, as shown below.

According to the Förster model,[30] the quenching efficiency is given by Equation (5):

$$E_m = \{1 + [2/(3\kappa_m^2](R_m/R_0)^6\}^{-1} \quad (5)$$

where R_m is the distance between the probes in the mth conformer, κ_m^2 a dimensionless geometric factor, which is written as[31, 32] Equation (6):

$$\kappa^2 = \cos^2\theta(3\cos^2\gamma + 1) \quad (6)$$

The two angles θ and γ determine the relative orientation of the donor and acceptor transition dipoles, and R_0 the Förster radius, that is the distance at which 50% transfer of excitation energy occurs [Eq. (7)].[23]

$$R_0 = 9.79 \times 10^3[(\tfrac{2}{3}\Phi_0 J_F)/n^4]^{1/6} \quad (7)$$

In Equation (7) Φ_0 is the quantum yield of the reference, n the refractive index of the solvent, and J_F (cm^2 mol^{-1}) the overlap integral [Eq. (8)]:

$$J_F = \frac{\int_0^\infty F_D(\bar{\nu})\varepsilon_A(\bar{\nu})\bar{\nu}^{-4}\,d\bar{\nu}}{\int_0^\infty F_D(\bar{\nu})\,d\bar{\nu}} \quad (8)$$

where $F_D(\bar{\nu})$ is the fluorescence intensity of the donor (Bin) and $\varepsilon_A(\bar{\nu})$ the extinction coefficient of the acceptor (Toac) at wavenumber $\bar{\nu}$.

From the spectral patterns and Equation (7), $R_0 = 9.7$ Å in methanol. Despite this relatively low value, the Förster model is adequate to describe the quenching process in the peptides examined, as suggested by the good agreement between theoretical and experimental quenching efficiencies reported in Table 5. Furthermore, it has been demonstrated that for a separation longer than 9 Å the rate takes the form expected for a pure dipole–dipole mechanism, while the exchange mechanism makes only a 5% contribution at 5 Å separation.[33] Several other papers support this conclusion,[11, 34] and recently the Dexter mechanism[35] has been shown to apply only to compounds exhibiting $R_0 = 5$ Å.[31] Therefore, in our case deviations from the Förster model should be definitely minor, if any.

Table 5. Molecular parameters of the low-energy B-T/*r*-*m* conformers and calculated and experimental quenching efficiencies in methanol.[a]

Peptide	R_m[b]	R_m'[c]	κ_m^2[d]	U_m[e]	% theor.	E_m[g] popul.[f]	E_i[h]
B-T/0-4	8.5	8.0	1.686	0.00	0.74	0.85	0.84
	8.5	8.1	0.009	0.63	0.25	0.03	≈ 0
	6.8	5.8	0.027	4.12	0.01	0.26	
B-T/1-3	9.7	9.2	0.300	0.00	0.89	0.31	0.28
	9.5	8.9	0.765	1.26	0.11	0.56	0.62
B-T/2-2	6.3	4.2	0.244	0.00	0.46	0.83	
	7.2	5.9	0.765	0.19	0.34	0.87	0.90
	7.3	6.0	0.019	0.50	0.20	0.14	0.09
B-T/3-1	7.2	5.2	0.685	0.00	0.56	0.86	
	9.2	8.0	0.479	0.40	0.29	0.50	0.47
	10.8	9.1	0.358	0.77	0.15	0.22	0.16

[a] The rows underlined refer to the hypothetical non-fluorescent ground-state complexes (see Figures 5 and 6). [b] Center-to-center distance [Å] in the mth conformer. [c] Center-to center distance between the NO$^\cdot$ group of Toac and π electron density of the closest naphthalene ring of Bin. [d] Orientation factor, from Eq. (6). [e] Relative energy [kcal mol^{-1}]. [f] Boltzmann weighted population. [g] Theoretical transfer efficiency, from Eq. (5). [h] Experimental transfer efficiency, from Eq. (2).

The computational results are summarized in Table 5, where the molecular parameters of the sterically most favoured right-handed 3_{10}-helical B-T/r-m peptides are listed. Besides the interprobe center-to-center distance, the distance between the NO$^\cdot$ group of Toac and the center of the π electron density in the closest naphthalene ring of Bin is reported in the same Table, together with both the theoretical and experimental transfer efficiencies.

The main inferences to be drawn from Table 5 are the following. First, in all cases the agreement between the calculated [E_m, Eq. (5)] and experimental [E_i, Eq. (2)] quenching efficiencies is very good only when the κ^2 orientation factor [Eq. (6)] is taken into account. This finding implies that the interconversion among conformational substates is definitely longer than the fluorescence decay, that is longer than 5 ns. Secondly, according to computational data, the conformational equilibria primarily involve the puckering of the Toac pyrrolidine moiety, where each substate is characterized by a different ring conformation. Thirdly, among the low-energy conformers there is one for each peptide, but B-T/1-3, exhibiting a NO$^\cdot$-naphthalene center-to-center distance < 6 Å, thus being a good candidate for the non-fluorescent complex responsible for the observed static quenching. Fourthly, the deepest energy minimum conformer of B-T/0-4 exhibits a peculiar and remarkably rigid geometry,

owing to the close proximity of Bin and Toac $C^{\alpha,\alpha}$-disubstituted Gly residues in the backbone chain. This allows the protons of the two free NH groups to experience a different environment, which is very likely responsible for the doublet observed in the NH stretching vibration region above 3400 cm^{-1} (Figure 2a). The proton of one of these groups, denoted as H'_{free}, is observed to be exposed to the solvent, while the other proton, denoted as H''_{free}, is buried in the peptide matrix, thus experiencing different van der Waals interactions, as illustrated in Figure 6.

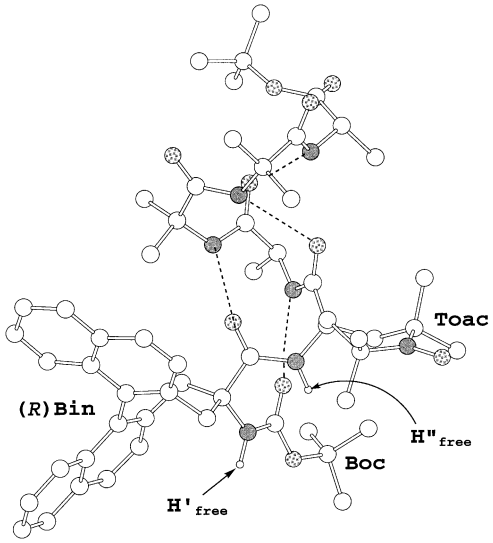

Figure 6. Molecular model of the deepest energy minimum conformer of B-T/0-4, viewed perpendicularly to the 3_{10} helix axis. The two NH protons, denoted as H'_{free} and H''_{free}, give rise to two IR absorption peaks within the 3410 – 3440 cm^{-1} wavenumber region, typical of the H-bond free NH stretching vibration (see Figure 2). The intramolecular hydrogen bonds are indicated by dashed lines. Nitrogen atoms are in black, oxygen atoms are dotted and hydrogen atoms are omitted for clarity.

Non-fluorescent and fluorescent low-energy conformers: The question now to address is how to theoretically identify the non-fluorescent complex, and which basic structural characteristics it does exhibit. One would expect a short interprobe separation distance, possibly shorter than anyone among the sterically most favoured structures of a given peptide, as required for electronic exchange interactions to occur.[33] In addition, the theoretical population of the non-fluorescent complex should be significantly lower than that experimentally evaluated,[36] because molecular mechanics underestimate electronic effects, which, on the contrary, are of paramount importance in the stabilization of this type of complex. These requirements are matched by only one low-energy conformer for each peptide examined, but B-T/1-3, as shown in Table 5, where the underlined rows refer to the molecular parameters of these hypothetical complexes. Interestingly enough, the negligibly small population of this complex of B-T/0-4 may be ascribed to the aforementioned conformational rigidity of this peptide, because a close approach of the chromophores can be only achieved by a partial twist of the helical backbone, which requires a high cost of energy (see Table 5).

Figures 7 and 8 illustrate the steric arrangement of the probes in the three sterically most favoured conformers of B-T/2-2 and B-T/3-1, respectively. In the case of B-T/2-2, the geometric arrangement of the probes in two conformers is such that a methyl group of Toac is found in between NO• and the closest naphthalene moiety of Bin (Figure 7a and b); this prevents static quenching despite the relatively short NO• – naphthalene center-to-center distance ($R_m' = 5.9$ Å). By contrast, the other low-energy conformer (Figure 7c) exhibits the shortest NO• – naphthalene center-to-center distance ($R_m' =$ 4.2 Å) and, at the same time, a free space in between these chromophores. The conditions for the occurrence of an

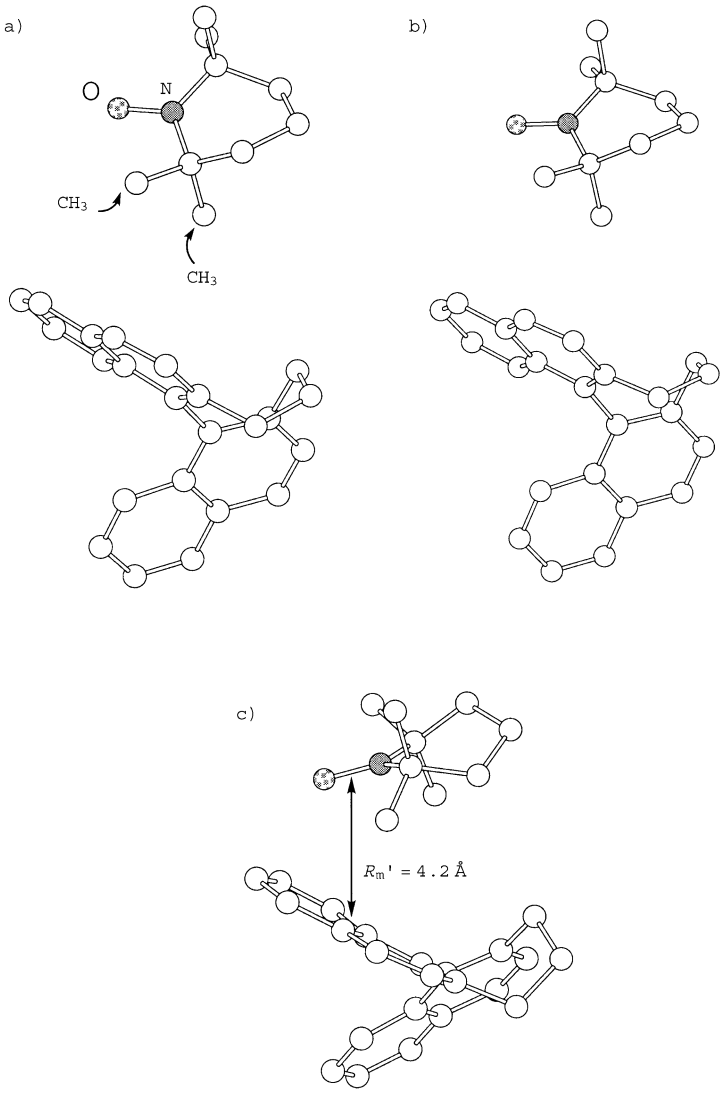

Figure 7. Steric arrangement of the chromophores in the deepest energy minimum conformer of B-T/2-2 (a) and in the next deepest one (b), along with the arrangement of the chromophores in the hypothetical non-fluorescent ground-state complex (c). In (a) and (b) a methyl group of Toac lies in between the two chromophores, while in (c) the close approach of the NO• moiety to one naphthalene ring of Bin can be easily envisaged. In the latter case, the very short center-to-center distance ($R_m' = 4.2$ Å, see Table 4) makes the occurrence of an instantaneous process between the active chromophores feasible. The 3_{10}-helical backbone chain is omitted for clarity. Nitrogen atoms are in black and oxygen atoms are dotted.

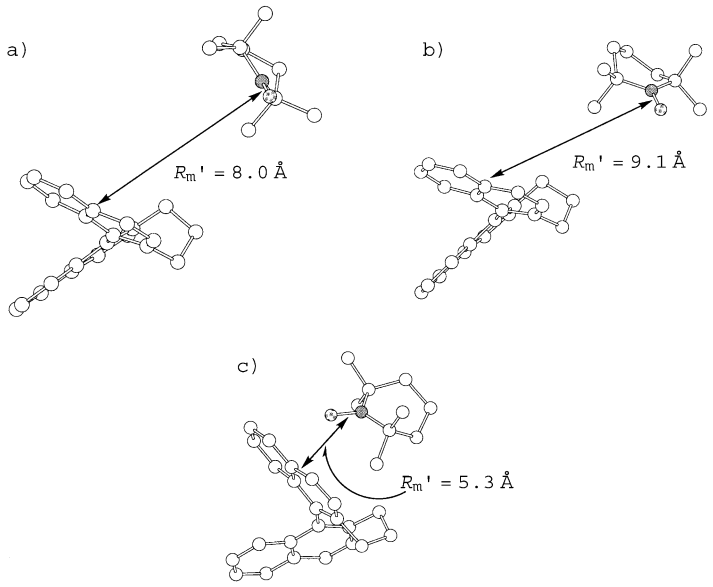

Figure 8. Steric arrangement of the chromophores in the deepest energy minimum conformer of B-T/3-1 (a) and in the next deepest one (b), along with the arrangement of the chromophores in the hypothetical non-fluorescent ground-state complex (c). The closest center-to-center distance between the naphthalene moiety of Bin and the NO· group of Toac is reported (R'_m; see also Table 4). The 3_{10}-helical backbone chain is omitted for clarity. Nitrogen atoms are in black and oxygen atoms are dotted.

instantaneous quenching process involving the chromophores are thus fulfilled. In the case of B-T/3-1, two low-energy conformers exhibit a relatively large NO·-naphthalene center-to-center distance (Figure 8a and b; $R_m' = 8.0$ and 9.1 Å), while the steric arrangement of the probes in the third conformer (Figure 8c) is such as to envisage it as the non-fluorescent complex ($R_m' = 5.3$ Å). On the basis of the different R_m' values, one would also expect a different population of the hypothetical non-fluorescent complexes of B-T/2-2 and B-T/3-1. This is indeed the case, the experimental population[33] is 85 and 59%, respectively, which, on the other hand, is predictably higher than the calculated population of the computed structures (around 15%).

Finally, as far as the sterically most favored conformers of B-T/1-3 are concerned, Figure 9 illustrates their molecular models, from which it clearly appears on a purely stereochemical ground that the non-fluorescent complex can not form, because in both conformers the chromophores are lying on the opposite side of the helix.

Conclusion

Combination of spectroscopic techniques (UV, CD, IR, nanosecond transient absorption, steady-state and time-resolved fluorescence) with molecular mechanics calculations allowed us to determine the most relevant structural features in solution of a set of conformationally restricted hexapeptides, carrying a rigid donor–acceptor pair. The compounds investigated populate very few conformers, all having the backbone chain in the right-handed 3_{10} helix. The analysis of time-resolved fluorescence measurements, based on the Förster energy transfer mechanism, suggests that the dynamics of interconversion among conformational substates is definitely slower than 5 ns. According to the molecular mechanics results, the substates equilibrium primarily involves the puckering of Toac piperidine ring, which controls the interprobe distance and hence the photophysical data. The photophysical behaviour of the conformations exhibiting a center-to center distance $R_{cc} > 6$ Å is determined by long-range dipolar interactions, leading to singlet–singlet energy transfer. By contrast, short-range exchange interactions are primarily involved in the conformers with $R_{cc} = 6$ Å, which leads to both non-fluorescent species and highly populated triplet states via EISC. Steric and electronic effects are thus responsible for the formation of the non-fluorescent complexes in the peptides investigated. In addition, exchange interactions are probably the main contributors to the $T_1 \rightarrow S_0$ relaxation, as measured by the T-T absorption time decays.

The overall findings made it possible to gain a better insight into the role played by steric constraints in the stabilization of ordered peptide conformations. These helical peptides are also good candidates as building blocks for a bottom-up generation of nanomolecular complex architectures with a well-defined structural organization.

Experimental Section

Materials: The Boc/O*t*Bu terminally protected, Bin/Toac hexapeptides were synthesized by solution methods and fully characterized. All peptide bond formations were achieved using the 1-[3-(dimethylamino)propyl]-3-ethyl-carbodiimide/7-aza-1-hydroxy-benzotriazole (EDC/HOAt) method.[37] All N^{α}-deprotection steps following Toac incorporation were carried

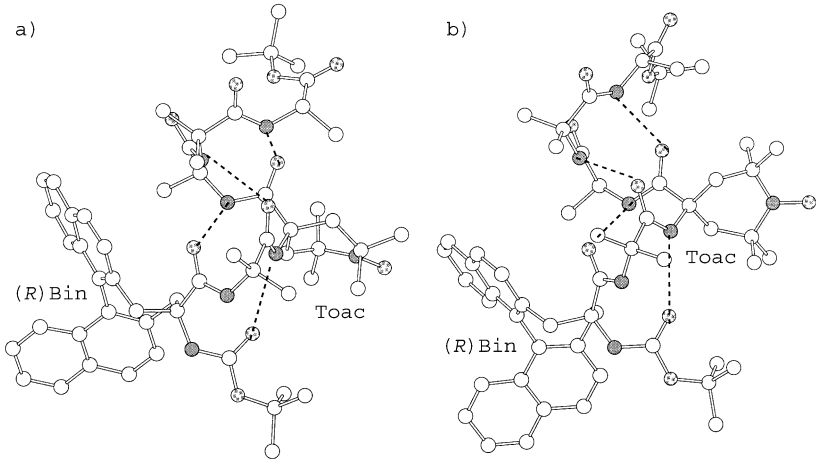

Figure 9. Theoretical model of the deepest energy minimum conformer of B-T/1-3 (a), and of the next deepest one (b), viewed perpendicularly to the right-handed 3_{10} helix axis. In both cases, the Bin and Toac chromophores are lying on the opposite side of the ordered backbone chain, thus preventing the formation of a non-fluorescent ground-state complex (see text). The intramolecular hydrogen bonds are indicated by dashed lines. Nitrogen atoms are in black, oxygen atoms are dotted and hydrogen atoms are omitted for clarity.

Table 6. Physical properties and analytical data for the terminally protected Bin/TOAC hexapeptides.

Compound		M.p.[a] [°C]	$[\alpha]_D^{20}$ [b]	TLC[c] R_f (I)	R_f (II)	R_f (III)	IR $\tilde{\nu}$ [cm^{-1}][d]
Boc-Bin-Toac-Ala-Aib-Aib-Ala-O*t*Bu	**(B-T/0-4)**	182–184	+20.4	0.85	0.95	0.25	3422, 3340,1760, 1672, 1526
Boc-Bin-Aib-Toac-Ala-Aib-Ala-O*t*Bu	**(B-T/1-3)**	185–185	+41.8	0.85	0.95	0.25	3424, 3330, 1731, 1669, 1529
Boc-Bin-Aib-Ala-Toac-Aib-Ala-O*t*Bu	**(B-T/2-2)**	230–231	+13.4	0.80	0.95	0.25	3425, 3317, 1729, 1666, 1529
Boc-Bin-Aib-Aib-Ala-Toac-Ala-O*t*Bu	**(B-T/3-1)**	179–181	+7.25	0.90	0.95	0.30	3425, 3321, 1733, 1667, 1530

[a] Determined on a Leitz model Laborlux 12 apparatus (Wetzlar, Germany). [b] Determined on a Perkin–Elmer model 241 polarimeter (Norwalk, CT) equipped with a Haake model L thermostat (Karlsruhe, Germany): $c = 0.5$ (methanol). [c] Silica gel plates (60F-254 Merck), solvent systems: I) chloroform/ethanol 9:1; II) butan-1-ol/water/acetic acid 3:1:1; III) toluene/ethanol 7:1; the plates were developed with a UV lamp or with the hypochlorite/starch/iodide chromatic reaction, as appropriate; a single spot was observed in each case. [d] Determined in KBr pellets on a Perkin–Elmer model 580B spectrophotometer equipped with a Perkin–Elmer model 3600 IR data station.

out on the fluoren-9-ylmethoxycarbonyl group. All intermediate and final compounds were obtained in a chromatographically homogeneous state. The physical properties and analytical data for the four hexapeptides are listed in Table 6. The reference derivative Boc-(*R*)-Bin-O*t*Bu was prepared from Boc-(*R*)-Bin-OH, resulting from N protection and successive saponification of H-(*R*)-Bin-OMe, previuosly obtained by resolution,[38a] as described in ref.[38b] for its *S* enantiomer. Spectrograde solvents (Fluka) were used, the deuterochloroform for IR spectra being 99.8% D.

Methods: Steady-state fluorescence spectra were recorded on a SPEX Fluoromax spectrofluorimeter, operating in SPC (single photon counting) mode. Quantum yields were obtained by using naphthalene in cyclohexane as reference ($\Phi_0 = 0.22$). Fluorescence decays were measured by a CD900 SPC apparatus from Edinburgh Instruments. Excitation in the UV region was achieved by using ultrapure hydrogen as filling gas. At the experimental conditions (300 mm Hg gas pressure. 30 kHz repetition rate) the FWHM (full width half maximum) of the excitation profile was 1.2 ns. The decay curves were fitted by a non-linear least-squares analysis to exponential functions by an iterative deconvolution method. All experiments were carried out in quartz cells using solutions previously bubbled for 20 min with ultrapure nitrogen.

Nanosecond transient absorption experiments were performed with an LKS.60 apparatus (Applied Photophysics, U.K.), using a Brilliant B Nd:YAG Q-switched laser (Quantel, France) equipped with a fourth harmonic generator module to obtain 266 nm excitation light with a pulse duration of 4 ns (FWHM) and an energy of about 10 mJ. Monochromatic probe light was obtained by filtering the output of a 150 W pulsed Xe lamp through two consecutive monochromators, positioned one before and the other behind the sample (bandpass 3 and 1 nm, respectively).

IR absorption spectra were recorded on a Perkin–Elmer model 1720X FT-IR spectrophotometer, nitrogen-flushed, equipped with a sample-shuttle device, at 2 cm^{-1} nominal resolution, averaging 100 scans.

Circular dichroism (CD) measurements were performed on a Jasco J-600 instrument with appropriate quartz cells.

Other apparatus were already described.[9, 39]

Acknowledgement

The financial support of both the Italian Research Council (CNR) and the Italian Interuniversity Consortium of Materials (INSTM) is gratefully acknowledged.

[1] S. M. Hecht, *Bioorganic Chemistry*: *Peptides and Proteins*, Oxford University Press, Oxford, **1998**.

[2] a) G. Yoder, A. Polese, R. A. G. D. Silva, F. Formaggio, M. Crisma, Q. B. Broxterman, J. Kamphuis, C. Toniolo, T. A. Keiderling, *J. Am. Chem. Soc.* **1997**, *119*, 10278–10285; b) T. S. Yokum, T. J. Gauthier, R. P. Hammer, M. L. McLaughlin, *J. Am. Chem. Soc.* **1997**, *119*, 1167–1168; c) I. L. Karle, *Acc. Chem. Res.* **1999**, *32*, 693–701; d) C. Toniolo, M. Crisma, F. Formaggio, C. Peggion, *Biopolymers (Pept. Sci.)* **2001**, *60*, 396–419.

[3] a) A. P. Winiski, M. Eisenberg, M. Langner, S. McLaughlin, *Biochemistry* **1988**, *27*, 386–392; b) F. S. Abrams, E. London, *Biochemistry* **1992**, *31*, 5312–5322; c) J. Matko, K. Ohki, M. Edidin, *Biochemistry* **1992**, *31*, 703–711; d) J. Matko, A. Jenei, L. Matyus, M. Ameloot, S. Damjanovic, *J. Photochem. Photobiol. B* **1993**, *19*, 69–73; e) J. Matko, A. Jenei, T. Wei, M. Edidin, *Cytometry* **1995**, *19*, 191–200.

[4] a) E. London, *Mol. Cell. Biochem.* **1982**, *45*, 181–188; b) A. P. Winiski, M. Eisenberg, A. Chattopadhyay, E. London, *Biochemistry* **1987**, *26*, 39–45; c) E. Asuncion-Punzalan, E. London, *Biochemistry* **1995**, *34*, 11460–11466.

[5] J. C. Scaiano, C. Paraskevopoulos, *Can. J. Chem.* **1984**, *62*, 2351–2358.

[6] J. Alvarez, E. A. Lissi, M. V. Encinas, *Langmuir* **1996**, *12*, 1738–1743.

[7] T. G. Traylor, V. S. Sharma, *Biochemistry* **1992**, *31*, 2847–2849.

[8] a) S. A. Green, D. J. Simpson, G. Zhou, P. S. Ho, N. V. Blough, *J. Am. Chem. Soc.* **1990**, *112*, 7337–7346; b) S. E. Herbelin, N. V. Blough, *J. Phys. Chem. B* **1998**, *102*, 8170–8176.

[9] B. Pispisa, A. Palleschi, L. Stella, M. Venanzi, C. Toniolo *J. Phys. Chem. B* **1998**, *102*, 7890–7898.

[10] M. Castanho, M. Prieto, *Biophys. J.* **1995**, *69*, 155–168.

[11] C. Toniolo, F. Formaggio, M. Crisma, J.-P. Mazaleyrat, M. Wakselman, C. George, J. R. Deschamps, J. L. Flippen-Anderson, B. Pispisa, M. Venanzi, A. Palleschi, *Chem. Eur. J.* **1999**, *5*, 2254–2264.

[12] a) T. Noyori, H. Takaya, *Acc. Chem. Res.* **1990**, *23*, 345–350; b) J. K. Whitesell, *Chem. Rev.* **1989**, *89*, 1581–1590.

[13] C. Toniolo, C. Benedetti, *Macromolecules* **1991**, *24*, 4004–4009.

[14] B. Pispisa, C. Mazzuca, A. Palleschi, L. Stella, M. Venanzi, F. Formaggio, C. Toniolo, J.-P. Mazaleyrat, M. Wakselman, *J. Fluoresc.* **2003**, *13*, 139–147.

[15] The ^{1}H NMR spectra of the Toac-containing peptides are not interpretable due to the line broadening effects induced by the paramagnetic nitroxide group.

[16] M. Rainaldi, Ph. D. Thesis, University of Padova, **2003**.

[17] a) N. Harada, K. Nakanishi, *Circular Dichroic Spectroscopy. Exciton Coupling in Organic Stereochemistry*, Oxford University Press, Oxford, **1983**; b) L. Di Bari, G. Pescitelli, P. Salvadori, *J. Am. Chem. Soc.* **1999**, *121*, 7998–8004; c) F. Formaggio, C. Peggion, M. Crisma, C. Toniolo, L. Tchertanov, J. Guilhem, J.-P. Mazaleyrat, Y. Goubard, A. Gaucher, M. Wakselman, *Helv. Chim. Acta* **2001**, *84*, 481–501.

[18] T. T. T. Bui, F. Formaggio, M. Crisma, V. Monaco, C. Toniolo, R. Hussain, G. Siligardi, *J. Chem. Soc. Perkin Trans. 2* **2000**, 1043–1052.

[19] R. W. Woody, in *Circular Dichroism*: *Principles and Applications* (Eds.: K. Nakanishi, N. Berova, R. W. Woody), VCH, New York, **1994**, pp. 473–496.

[20] S. Mizushima, T. Shimanouchi, M. Tsuboi, R. Souda, *J. Am. Chem. Soc.* **1952**, *74*, 270–271.

[21] G. M. Bonora, C. Mapelli, C. Toniolo, R. R. Wilkening, E. S. Stevens, *Int. J. Biol. Macromol.* **1984**, *6*, 179–188.

[22] B. Pispisa, A. Palleschi, L. Stella, M. Venanzi, C. Mazzuca, F. Formaggio, C. Toniolo, Q. B. Broxterman, *J. Phys. Chem. B* **2002**, *106*, 5733–5738.

[23] J. R. Lakowicz, *Principles of Fluorescence Spectroscopy*, Kluwer, New York, **1999**.

[24] Y. Kobori, A. Kawai, K. Obi *J. Phys. Chem.* **1994**, *98*, 6425–6429.

[25] J. B. Birks, *Photophysics of Aromatic Molecules*, Wiley, New York, **1970**.

[26] a) C. Corvaja, E. Sartori, A. Toffoletti, F. Formaggio, M. Crisma, C. Toniolo, J.-P. Mazaleyrat, M. Wakselman, *Chem. Eur. J.* **2000**, *6*, 2775–2782; b) C. Corvaja, E. Sartori, A. Toffoletti, F. Formaggio, M. Crisma, C. Toniolo, *Biopolymers (Pept. Sci.)* **2000**, *55*, 486–495.
[27] a) B. Pispisa, A. Palleschi, *Macromolecules* **1986**, *19*, 904–912; b) B. Pispisa, M. Venanzi, A. Palleschi, G. Zanotti, *Biopolymers* **1995**, *36*, 497–510; c) B. Pispisa, M. Venanzi, A. Palleschi, G. Zanotti, *J. Phys. Chem.* **1996**, *100*, 6835–6844; d) B. Pispisa, L. Stella, M. Venanzi, A. Palleschi, F. Marchiori, A. Polese, C. Toniolo, *Biopolymers* **2000**, *53*, 169–181; e) B. Pispisa, A. Palleschi, C. Mazzuca, L. Stella, A. Valeri, M. Venanzi, F. Formaggio, C. Toniolo, Q. B. Broxterman *J. Fluoresc.* **2002**, *12*, 213–217.
[28] W. L. Mattice, U. W. Suter, *Conformational Theory of Large Molecules*, Wiley, New York, **1994**.
[29] G. Némethy, M. S. Pottle, H. A. Scheraga, *J. Phys. Chem.* **1983**, *87*, 1883–1887.
[30] a) T. Förster, *Ann. Phys. (Leipzig)* **1948**, *2*, 55–75; b) T. Förster, *Discuss. Faraday Soc.* **1959**, *27*, 7–17.
[31] B. W. van der Meer, in *Resonance Energy Transfer* (Eds.: D. L. Andrews, A. A. Demidov), Wiley, New York, **1999**, pp. 151–172.
[32] B. Pispisa, M. Venanzi, A. Palleschi, G. Zanotti, *J. Photochem. Photobiol. A*: *Chem.* **1997**, *105*, 225–233.
[33] a) G. D. Scholes, K. P. Ghiggino, A. N. Oliver, M. N. Paddon-Row, *J. Am. Chem. Soc.* **1993**, *115*, 4345–4349; b) G. D. Scholes, K.P Ghiggino, *J. Phys. Chem.* **1994**, *98*, 4580–4590; c) G. D. Scholes, K. P. Ghiggino, *J.Photochem. Photobiol. A*: *Chem.* **1994**, *80*, 355–362.
[34] a) J. A. Green II, L. A. Singer, J. H. Parks, *J. Chem. Phys.* **1973**, *58*, 2690–2695; b) S.-T. Levy, M. B. Rubin, S. Speiser, *J. Am. Chem. Soc.* **1992**, *114*, 10747–10756; c) S.-T. Levy, S. Speiser, *J. Chem. Phys.* **1992**, *96*, 3585–3592.
[35] D. L. Dexter, *J. Chem. Phys.* **1953**, *21*, 836–850.
[36] The experimental population of the non-fluorescent ground-state complex can be evaluated by the expression $[(E - \langle E\rangle)/(1 - \langle E\rangle)]$, where $E = [1 - (\Phi/\Phi_0]$ and $\langle E\rangle = [1 - (\langle\tau\rangle/\tau_0]$.
[37] L. A. Carpino, *J. Am. Chem. Soc.* **1993**, *115*, 4397–4398.
[38] a) J.-P. Mazaleyrat, A. Boutboul, Y. Lebars, A. Gaucher, M. Wakselman, *Tetrahedron*: *Asymmetry* **1998**, *9*, 2701–2713; b) J.-P. Mazaleyrat, A. Gaucher, J. Savrda, M. Wakselman, *Tetrahedron*: *Asymmetry* **1997**, *8*, 619–631.
[39] B. Pispisa, M. Venanzi, L. Stella, A. Palleschi, G. Zanotti, *J. Phys. Chem. B* **1999**, *103*, 8172–8179.

Received: January 10, 2003 [F4727]

